

## Hubbard Glacier, Alaska: 2002 closure and outburst of Russell Fjord and postflood conditions at Gilbert Point

Roman J. Motyka<sup>1</sup> and Martin Truffer<sup>1</sup>

Received 10 February 2006; revised 2 October 2006; accepted 4 December 2006; published 14 April 2007.

[1] Hubbard Glacier, the largest temperate tidewater glacier in the world, has been advancing since 1895 AD and has now twice dammed 60-km-long Russell Fjord, once in 1986 and more recently in 2002. This paper focuses on the 2002 event, when a strong spring advance pushed shallow submarine proglacial sediments against Gilbert Point, closing off Russell Fjord by late June. As a consequence, upstream ice flow decelerated from  $5 \text{ m d}^{-1}$  to  $1.5 \text{ m d}^{-1}$ , with flow diverging to either side of Gilbert Point. Lake height reached 15 m asl before intense rains caused lake water to overtop the moraine dam on 14 August 2002. Three cubic kilometers of water were released within 30 hours, with peak discharge reaching  $55,000 \text{ m}^3 \text{ s}^{-1}$  24 hours after the flood began. The discharge records for the 1986 and 2002 outbursts differ significantly and reflect differences in lake height (26 m versus 15 m) and dam types (ice versus moraine). The 2002 outburst proceeded in two stages: (1) relatively slow overtopping of the subaerial moraine with downward erosion rates of  $1\text{--}2 \text{ m h}^{-1}$  with little lateral expansion, (2) followed by faster downward erosion of the submarine moraine (up to  $7 \text{ m h}^{-1}$ ) with rapid lateral expansion of the channel by ice calving ( $\sim 7 \text{ m h}^{-1}$ ). The annual average terminus position at Gilbert Point has remained constant since 2002, although there are seasonal variations of 100–200 m. The deep channel, strong tidal currents, and seasonally warm ocean water appear to have prevented the advance of this segment of the terminus despite the glacier's continued advance elsewhere along its terminus. Sediments are slowly filling in the channel at a rate of about  $4 \text{ m yr}^{-1}$ , and their steady accumulation may eventually trigger the next closure.

**Citation:** Motyka, R. J., and M. Truffer (2007), Hubbard Glacier, Alaska: 2002 closure and outburst of Russell Fjord and postflood conditions at Gilbert Point, *J. Geophys. Res.*, 112, F02004, doi:10.1029/2006JF000475.

### 1. Introduction

[2] Hubbard Glacier, located near Yakutat, Alaska (Figure 1), is the largest nonpolar tidewater glacier in the world and has advanced over 2.5 km during the last century. This advance has now brought the terminus close to Gilbert Point at the entrance to 60-km-long Russell Fjord (Figure 2). Hubbard Glacier has dammed Russell Fjord twice in historic times, once in 1986 and again in 2002. Both dams failed catastrophically. These closures and subsequent floods are among the most significant glaciological events in North America in recent decades. The 1986 event was the subject of several articles [Seitz *et al.*, 1986; Mayo, 1988, 1989; Trabant *et al.*, 1991; Krimmel and Trabant, 1992] and received widespread attention in the press. Although the 2002 closure was also well publicized and well documented by photos and additional observations, it has only been cursorily described in the scientific literature [Trabant *et al.*, 2003a, 2003b]. Trabant *et al.* [2003a] also

summarized the state of the Hubbard terminus as of 2001. Our examination of the 2002 event builds on these earlier studies and relies heavily on information gathered by a number of government agencies and private individuals as well as our own postoutburst investigations.

[3] Most studies of glacier-dammed lakes have focused on ice marginal freshwater lakes [e.g., Walder and Costa, 1996; Anderson *et al.*, 2003] or subglacial geothermal lakes [e.g., Björnsson, 2002] (see also Roberts [2005] for a review). The advance of Perito Moreno Glacier, a lacustrine calving glacier in Argentina, has periodically blocked a large tributary arm of the lake with dam failures there producing outburst floods that are reported to have released 3 to 4 km<sup>3</sup> of water [Skvarca and Naruse, 2006; Stueffer *et al.*, 2007]. However, to our knowledge, Hubbard Glacier is the first historic instance of an advancing tidewater glacier damming a major waterway. Tidewater glacier dynamics can add additional complexity to the evolution and destruction of dams and the observations at Hubbard Glacier allow us to examine various factors involved including calving and submarine melting and their dependence on water depth, ocean temperature, tidal currents, and sediment mobilization. Observations and flood records from 2002 also allow us to develop and test a model of dam failure and

<sup>1</sup>Geophysical Institute, University of Alaska Fairbanks, Fairbanks, Alaska, USA.

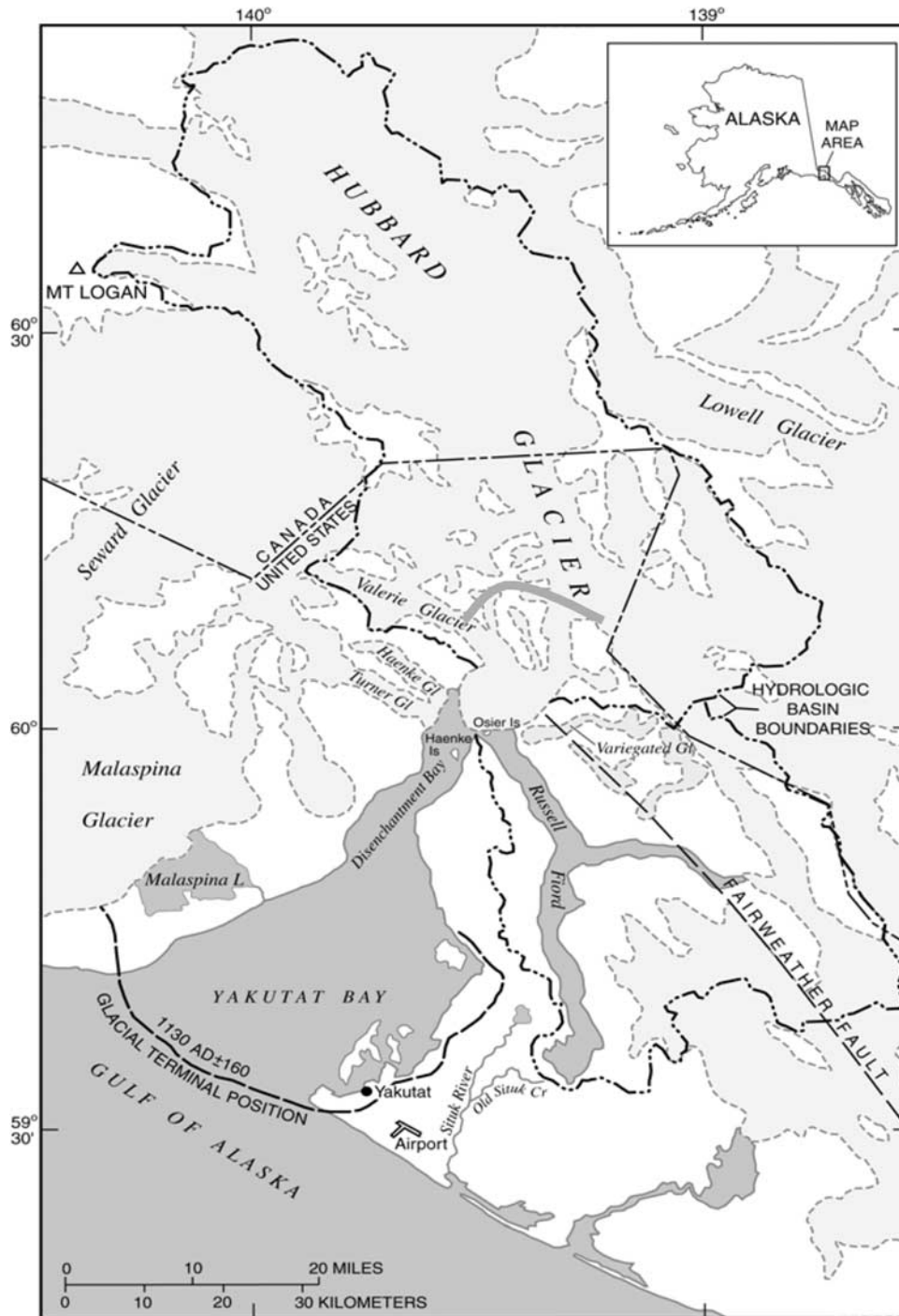


**Figure 1.** Map of study area (modified from [Trabant *et al.*, 2003b]). In the early 1100s, Hubbard Glacier was in an advanced state, to the Gulf of Alaska and the modern town of Yakutat. Around 1300 AD it started a retreat into Yakutat Bay that lasted through the entire Little Ice Age (LIA). The glacier has advanced 2.5 km since 1895, despite the widespread glacier recession in the area. Hubbard Glacier’s equilibrium line altitude (ELA, gray line indicates approximate position) is located in a relatively steep section, making the glacier less sensitive to ongoing or future climate change. Currently, the glacier leaves only a small gap (~300 m in summer 2004) between itself and Gilbert Point. Russell Fjord is currently connected to Disenchantment Bay by this tidal channel.

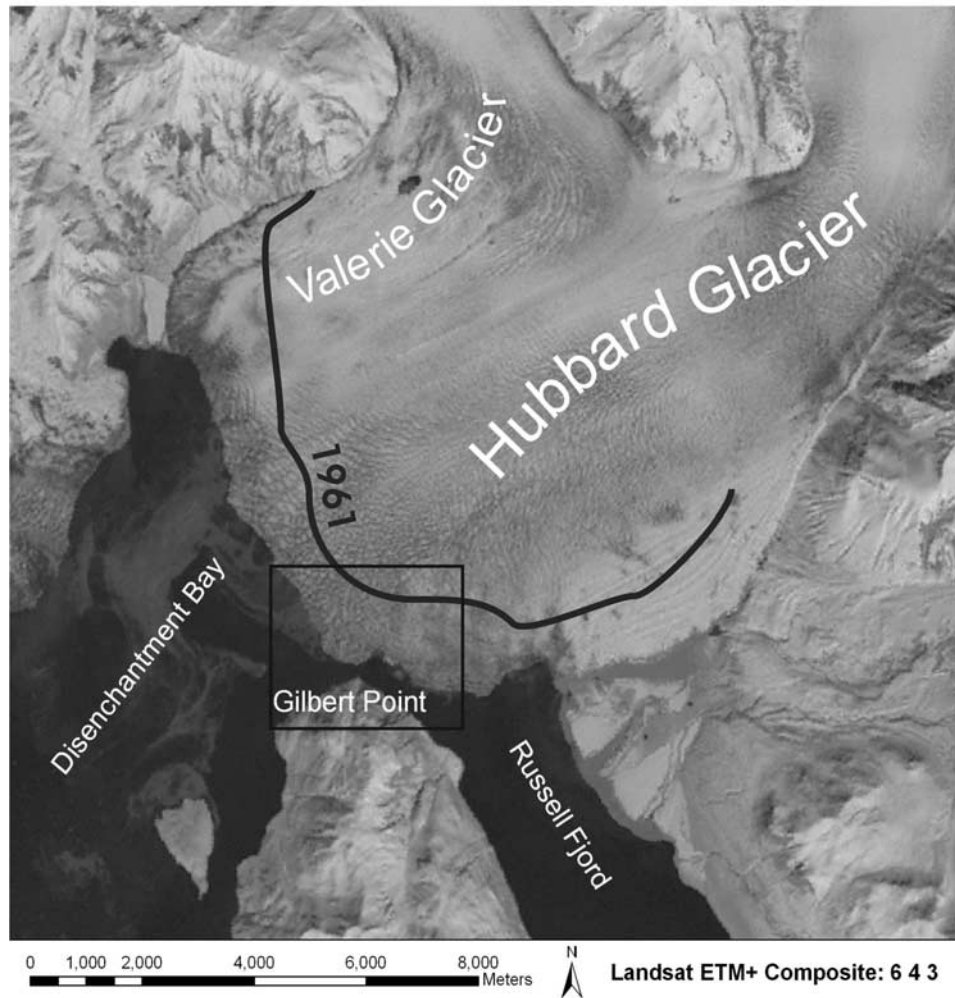


**Figure 2.** Landsat image of terminus position of Hubbard Glacier on 1 October 2000. Terminus position in 1961 shown by black boundary. Generally, the glacier has steadily advanced but has seasonal oscillations of 100–200 m. A more complicated picture presents itself around Gilbert Point, where the 2002 outburst flood substantially eroded the ice face and caused a local retreat. Boxed area roughly defines region of ice flow analysis.

outburst discharge [e.g., *Walder and Costa, 1996; Walder and O'Connor, 1997*]. The collision of an advancing glacier with a rock wall is a rarely witnessed event, much less documented and quantified. At Gilbert Point (Figure 2) it significantly affected upstream ice flow and stability of the glacier dam itself. Lastly, understanding the dynamics in this region is important for assessing the factors facilitating another closure, the timing of the next closure, and the stability of any future dams.

[4] In this paper we describe Hubbard Glacier; discuss the formation of the 2002 dam and the subsequent outburst flood; analyze the changes in ice flow patterns caused by this event; show changes in bathymetry in and around the point of dam formation; present a discharge model for the outburst flood; and finally discuss how channel depth and warm ocean temperatures may be preventing the glacier from readvancing and closing Russell Fjord since 2002. The last of these has implications for the future behavior of the glacier. Future closures are of serious concern to residents of

the nearby town of Yakutat because rising lake level could breach a 41-m low point at the southern end of Russell Fjord (Figure 1). The resulting drainage would affect the Situk River fishery, road systems, structures, and municipal airport. Although both previous dams failed before water could breach the southern low point, future dams could hold and cause spillover.

## 2. Hubbard Glacier and Gilbert Point

[5] Heading on flanks of Mount Logan in Canada (5959 m), Hubbard Glacier covers an area of 3500 km<sup>2</sup> and flows over 120 km to sea level where its 11.5 km wide terminus calves into Disenchantment Bay and Russell Fjord (Figures 1 and 2). Hubbard Glacier is an excellent example of how a tidewater glacier can behave asynchronously with neighboring glaciers and independently of climate. While glaciers in southern Alaska were advancing during the Little Ice Age, Hubbard Glacier underwent a dramatic retreat

[Barclay *et al.*, 2001]. In contrast, it has now advanced 2.5 km since 1895 [Trabant *et al.*, 2003a], a period when glaciers in the surrounding region have been losing mass, some of them at increasing rates [Arendt *et al.*, 2002; Larsen *et al.*, 2007]. The current advance of Hubbard Glacier is driven by its very high ratio of accumulation to total area (AAR) of 0.95, and we consider the glacier to be in the advance phase of the so-called tidewater glacier cycle [Post, 1975; Meier and Post, 1987; Post and Motyka, 1995; Trabant *et al.*, 2003a].

[6] The time and width-averaged glacier advance between 1986 and 2002 was  $28 \text{ m yr}^{-1}$  into Disenchantment Bay and  $34 \text{ m yr}^{-1}$  into Russell Fjord. This long-term advance has a strong seasonal cycle with advance in winter to spring and retreat in summer to fall with oscillations as large as 100 to 200 m [Trabant *et al.*, 1991; Ritchie *et al.*, 2006]. The surface elevation has also been slowly increasing, particularly at lower elevations, at rates of about  $1\text{--}2 \text{ m yr}^{-1}$  [Trabant *et al.*, 2003a]. The terminus is grounded on a submarine moraine that lies about 90 m below sea level (bsl) in Disenchantment Bay and Russell Fjord [NOAA, 2000].

[7] A sparse set of radio echo soundings (RES) in 1986–1988 showed the glacier to be about 360 m thick along the centerline with the bed at 180 m bsl at a distance of 1 km upstream from the terminus [Trabant *et al.*, 1991]. Ice thickness increases to 800 m and bed depth drops to 400 m bsl at 3 km. Trabant *et al.* [2003a] reported near-terminus centerline speeds of  $11.5 \text{ m d}^{-1}$  during the summer of 2001 and seasonal velocity variations in the terminus lobe of up to  $2 \text{ m d}^{-1}$ , slowing down in late summer.

[8] This paper focuses on the region near Gilbert Point where two closures and outbursts have already occurred and where continued glacier advance threatens further closures of 60-km-long Russell Fjord (Figure 2). On the Russell Fjord side, Trabant *et al.* [1991] reported near terminus ice thickness of about 140 m with the bed  $\sim 85 \text{ m bsl}$ . Ice flow in this region is much slower than at the centerline, averaging about  $5\text{--}6 \text{ m d}^{-1}$  during the 1990s (R. M. Krimmel, unpublished data). Archival NOAA charts [NOAA, 1984] show that the regions seaward of the Gilbert Point shoreline were very shallow in 1977, with water depths less than 2 m in places, and that the glacier terminus was within 50 m of these reefs (see also Figure 8a). In 1986, the glacier crossed this shallow region, closing off Russell Fjord in June [Mayo, 1988]. The subsequent outburst in October 1986 is the largest outburst flood on record, achieving nearly twice the highest peak flow of the Mississippi River [Mayo, 1989]. The 1986 outburst stripped the sediments from Gilbert Point to depths exceeding 35 m [Trabant *et al.*, 1991] and redeposited them in Disenchantment Bay [Cowen *et al.*, 1996], appreciably deepening the tidal channel and widening it to 300 m. Channel width was still about 300 to 400 m in 1999 and water depths averaged about 25 m.

[9] Despite predictions of imminent glacier readvance and damming [Trabant *et al.*, 1991], the next closure did not occur until 2002. During the intervening years, glacier advance averaged only  $6 \text{ m yr}^{-1}$  toward Gilbert Point [Ritchie *et al.*, 2006], much less than predicted and much less than elsewhere along the terminus. However, by May 2002 the glacier once again began pushing up sediments

above sea level and continued advancing toward Gilbert Point, blocking Russell Fjord by mid-June.

### 3. Methods

#### 3.1. Sources of Data on the 2002 Closure and Outburst Flood

[10] Our chronology of the 2002 closure and outburst of Russell “Lake” is largely based on photos and observations obtained by multiple governmental agencies and private individuals that were monitoring the situation (<http://www.fs.fed.us/r10/tongass/hubbard>; <http://ak.water.usgs.gov/glaciology/hubbard/>), as well as our own observations. Other data sources are high-resolution (1:6000), low-elevation vertical aerial photos that were acquired for the National Marine Fisheries Service (NMFS) as part of their study of seal populations on icebergs in Disenchantment Bay. These surveys serendipitously overlapped with the 2002 damming of Russell Fjord. The aerial photos included the glacier terminus and were taken periodically from early May through August including during and immediately after the outburst flood. Although the photos lacked stereo coverage, we were nevertheless able to measure terminus boundaries, moraine growth, and horizontal glacier flow in the vicinity of Gilbert Point.

[11] The water level record for “Russell Lake” was obtained from the U.S. Geological Survey (USGS) who operated a standard water level type tide gauge located in the “lake”. Measurements were corrected to mean sea level datum and the accuracy of the manometer is  $\pm 0.003 \text{ m}$  [Seitz *et al.*, 1986].

#### 3.2. Ice Flow

[12] Sequential vertical aerial photography has been previously used to measure surface ice velocities [e.g., Krimmel, 2001]. At Hubbard, we determined horizontal ice and moraine surface movement in the vicinity of Gilbert Point during the summer of 2002 using photogrammetric analysis and feature tracking on relatively low-elevation vertical aerial photos. Six sets of photos comprised the database: 2 May, 7 June, 7 July, 14 August, 16 August, and 23 August. Because the photos lack stereo overlap (preventing DEM creation), we used other procedures to extract the best position data for feature tracking. The primary adjustments were for terrain height and camera position. The photo sets were taken from nearly identical elevations and orientations, and the frames were shot from nearly identical locations, facilitating analysis. Adjustments were made for differences in scale and photo orientation between the photo sets. Corrections for terrain height (essentially orthorectification) were facilitated by a lidar survey of the ice surface near Gilbert Point acquired on 16 August 2002 (R. Gubernick, USFS, unpublished data, 2003). The time-averaged horizontal velocity  $\bar{U}$  and flow direction,  $\theta$ , of a surface feature were computed from:

$$\bar{U} = \Delta H / \Delta t \quad \text{and} \quad \theta = \arctan(\Delta y / \Delta x) \quad (1)$$

where  $\Delta y$  and  $\Delta x$  are the changes in horizontal coordinates in a 2-D Cartesian reference frame,  $\Delta H$  is the change in horizontal position of the feature, and  $\Delta t$  is the time interval between photos.

[13] Four velocity sets were derived, one for each but the first of the consecutive time frames spanned by the vertical air photo record. It was not possible to co-identify features on the 2 May and 7 June photos because of snow cover. Terminus and moraine boundaries were derived from all photo sets. Our analysis was restricted to the regions close to Gilbert Point covering an area of about 3 km<sup>2</sup> (Figure 2). Photo coverage barely extended into Russell Fjord and did not extend up glacier. Regions westward along the terminus into Disenchantment Bay lacked shoreline control necessary for photogrammetric analysis.

[14] Uncertainties in our velocity calculations are due to uncertainties in the estimates of feature elevation ( $\pm 15$  m), resolution of position ( $\pm 0.5$  to 3 m), and uncertainties in adjustments for differences in photo scale and orientation between photo sets. Photo dates and times are known to within a minute and therefore uncertainties in  $\Delta t$  are negligible. The magnitudes of uncertainties due to each of the previous factors vary as a function of the position of the feature on the photo. We therefore computed the combined uncertainty separately for each velocity using error propagation.

### 3.3. Bathymetry

[15] Acquiring bathymetric data became a priority of our investigation in the aftermath of the 2002 event. Water depth is thought to be a key factor in controlling tidewater glacier stability and calving rates appear to be at least partially a function of water depth [Post, 1975; Brown *et al.*, 1982; Meier and Post, 1987; van der Veen, 1996; Motyka *et al.*, 2003]. Knowledge of water depths is also essential for assessing stability of ice dams because ice flotation can trigger subglacial release of jökulhlaups [Björnsson, 1992, 2002; Roberts, 2005]. Temporal and spatial changes in water depth reflect deposition or erosion of proglacial sediments, which in turn can lead to increased or decreased terminus stability.

[16] Bathymetric surveys of the area were conducted by the National Ocean Survey (NOS) in 1977–1978 [NOAA, 1984] and 1999 [NOAA, 2000]. We used the earlier chart as a basis of comparison for later changes. We also obtained the NOS 1999 survey data (<http://www.oceanservice.noaa.gov/dataexplorer/>) surrounding Gilbert Point and derived a bathymetric baseline to compare to post-2002 outburst data.

[17] Because of limited resources, we restricted our own surveys to regions of Disenchantment Bay and Russell Fjord near Gilbert Point, the site of past and potentially future closures. We used a narrow beam ( $6^\circ$ ) 1 kW depth sounder to measure water depths in the vicinity of Gilbert Point on 23 August 2002, 9 days after the outburst started and then annually in late summer through 2005. The depth sounder was calibrated in situ against known water depths. The estimated accuracy of raw water depth measurements is on the order of 0.5 m. The bathymetry data were coregistered and logged with GPS data at 5 s intervals. This completely portable system was installed on a 20 foot skiff. Post processing against a base station in Yakutat ensured positional accuracy of  $\pm 1$  m or better. Raw water depth data were corrected for tidal stages based on tidal corrections made during a NOS survey of the area in 1999. All water depths are given with respect to mean lower low water (MLLW) (the height of the lower of the two low tide levels

over a tide cycle averaged over a 19-year period), which is standard practice for bathymetric charts. The difference between MLLW and mean sea level is about 2.2 m, estimated from the tide record at nearby Yakutat. Given that tidal corrections in the vicinity of Gilbert Point have likely changed somewhat over time since the 1999 NOS survey, overall uncertainties of our water depth surveys are about  $\pm 1.5$  m.

### 3.4. Water Temperature

[18] Some studies indicate that ocean water temperatures can play a significant role in the mass balance and stability of a tidewater terminus through submarine melting [e.g., Walters *et al.*, 1988; Motyka *et al.*, 2003]. Water temperature can also play a role during an outburst flood from a glacier-dammed lake because water above  $0^\circ\text{C}$  can melt ice and widen the outflow channel [Walder and Costa, 1996]. We therefore measured ocean water temperatures as a function of depth during each of our annual bathymetric surveys as well as on 23 April 2003 using submersible temperature loggers, accurate to  $\pm 0.2^\circ\text{C}$ . These measurements were primarily made in eastern Disenchantment Bay (EDB).

## 4. Results

### 4.1. Evolution of the 2002 Dam

[19] The first visible sign that closure was imminent was the emergence of proglacial sediment above water in front of the glacier terminus, visible on 2 May 2002. The glacier was then 190 m from Gilbert Point. The glacier advanced 40 m toward Gilbert Point during May and early June, pushing submarine moraine sediments forward with shoaling visible along a 0.5 km arc of the terminus (Figure 3a). The shoal moraine effectively shut down ice calving and narrowed the channel between Disenchantment Bay and Russell Fjord to 75 m.

[20] The glacier advanced another 130 m through June, shoving the moraine against Gilbert Point in a series of imbricate thrusts and closed off the fjord entirely by mid-June. Water level began rising in the newly forming “Russell Lake”. The moraine was 5 m (asl) high and formed a 50 m wide dam at Gilbert Point by 7 July 2002 (Figure 3b). A small stream along the rock wall drained through the moraine from the newly formed lake. Moraine height continued to increase through July, keeping pace with rising lake level. Figure 4 (10 August 2002) captures the full extent of the moraine and ice dam prior to the outburst. The moraine at the drainage channel was 14 m asl. Ice upstream of the dam came within 10 m of the rock wall and threatened to also close the gap there.

### 4.2. Lake Level Rise and Outburst

[21] Table 1 provides a chronology of events during the 2002 outburst flood. Lake level rose at a relatively steady rate of about  $0.2\text{ m d}^{-1}$  during water impoundment but three days of intense rain beginning on 12 August accelerated lake level rise to  $\sim 1\text{ m d}^{-1}$  (Figure 5). Water rise soon outpaced the rise in moraine height and breached the moraine dam. The dam began to fail shortly after midnight on 14 August as captured by water level measurements (Figure 5 and Table 1). We derived a discharge curve as

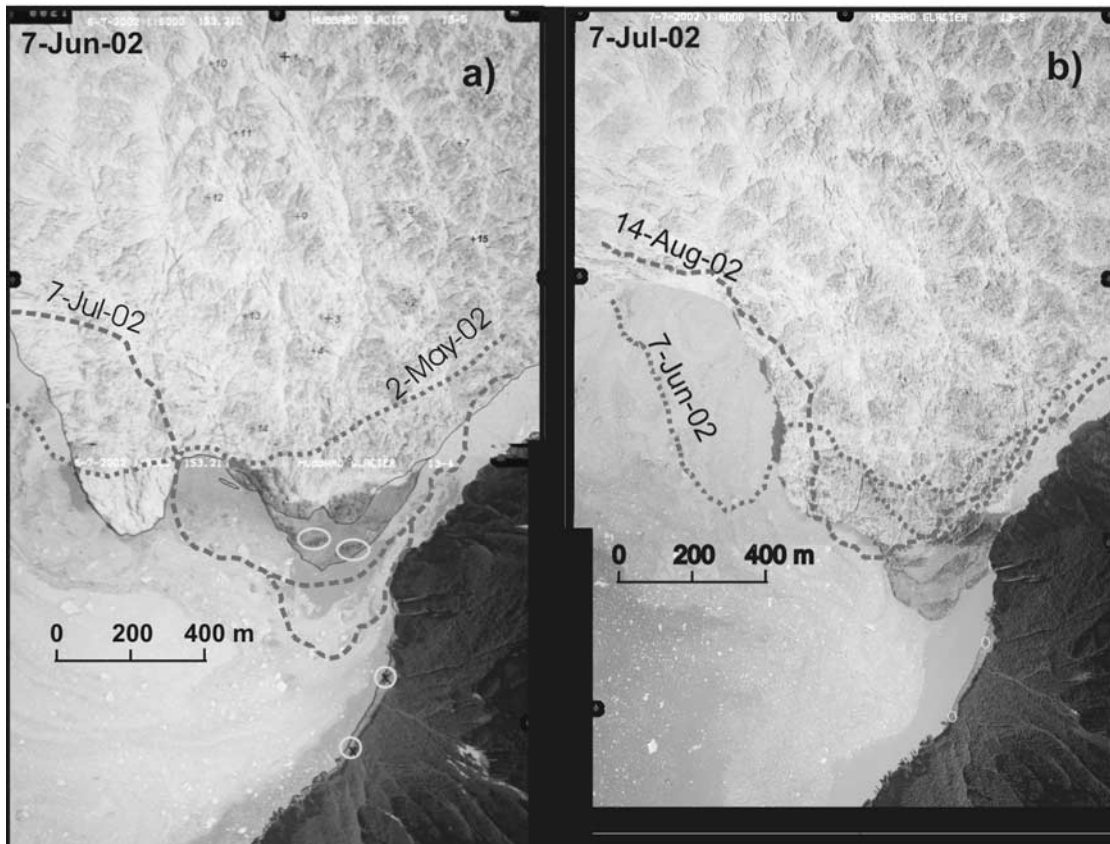


**Figure 3.** NMFS vertical air photo mosaic of Gilbert Point dam (a) on 7 June 2002 and (b) on 7 July 2002. Glacier and moraine boundaries from preceding photo are shown by dashed line.



**Figure 4.** Photo (National Park Service), taken 4 days before dam rupture, that captures the full extent of the moraine and ice dam prior to the outburst. The moraine has been squeezed up against Gilbert Point, increasing in elevation to 14 m asl. Ice was also threatening to close the ~10 m gap behind the moraine dam.

**Table 1.** Chronology of 2002 Hubbard Glacier Outburst Flood

Data Source	Time, ADT	Average Width, m	Comments
Oblique photo record	10 Aug 2002; 1300	0	moraine dam fully formed
Discharge record	14 Aug 2002; 0000	0	outburst begins
Oblique photo record	14 Aug 2002; 1200	70 ± 10	discharge controlled by moraine
Discharge record	14 Aug 2002; 1330	-	inflection in discharge curve
NMFS vertical photo	14 Aug 2002; 1622	117 ± 5	glacier calving and erosion widen gap
Oblique photo record	14 Aug 2002; 1715	-	moraine totally gone
Oblique photo record	14 Aug 2002; 1930	134 ± 20	last photo record of discharge
Discharge record	15 Aug 2002; 0015	-	peak discharge
Discharge record	15 Aug 2002; 1230	-	end of outburst projected from discharge curve
NMFS vertical photo	16 Aug 2002; 1649	235 ± 10	channel appreciably widened
GPS overflight	25 Aug 2002; 1000	230 ± 20	width stable
NMFS vertical photo	26 Aug 2002; 1454	250 ± 20	width stable

shown in Figure 6 by differencing the water level data during the outburst period, using methods and fjord hypsometry described by Mayo [1989].

[22] Discharge was relatively slow at first but sufficient to begin eroding the moraine dam. Discharge increased as erosion accelerated, with the moraine dam completely gone by 17:15 h. The inflection in the discharge curve marks an acceleration in discharge as water flow and ice calving began eroding the ice cliff, widening the outburst channel to 135 m. Discharge peaked at  $55,000 \text{ m}^3 \text{ s}^{-1}$  at about midnight with the lake draining to sea level by midday 15 August (Figures 5 and 6).  $3 \text{ km}^3$  of water flushed through the gap in a period of about 30 hours. Only a small remnant of the moraine remained above water in the aftermath. Ice calving had widened the channel to  $\sim 230 \text{ m}$  by the next day (Table 1 and see Figure 7d).

#### 4.3. Ice Velocities

[23] Figure 7 shows the derived velocity fields for four time periods, spanning the time of dam building, dam

collapse, and postoutburst recovery. The ellipses depict the estimated errors. The greater uncertainties in the last two periods reflect the short time interval between observations.

[24] Figure 7a shows the average ice velocity field during the period when the glacier and moraine dam were first being formed. Flow into Eastern Disenchantment Bay (EDB) averaged about  $11\text{--}12 \text{ m d}^{-1}$  and  $4\text{--}6 \text{ m d}^{-1}$  on the eastern side of the gap. The flow vectors show strong N–S shear and prominent E–W compression toward Gilbert Point. The proglacial moraine was being pushed forward uniformly at about  $4 \text{ m d}^{-1}$ , nearly identical to terminus ice flow at this location.

[25] By July, speeds decelerated by a factor of two or more throughout the study area:  $5\text{--}6 \text{ m d}^{-1}$  into EDB and  $1.5 \text{ m d}^{-1}$  toward Gilbert Point (Figure 7b). Flow was also becoming more bifurcated to either side of Gilbert Point. The collision of the moraine against Gilbert Point was now not only impounding water in Russell Lake but also damming upstream ice and producing a flow divide. This

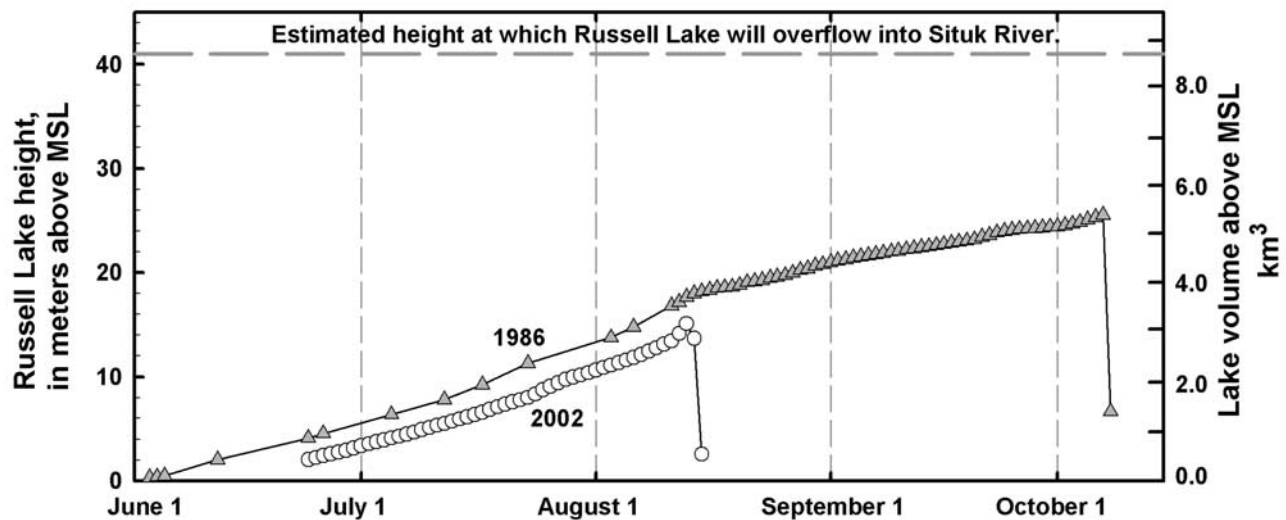


**Figure 5.** Comparison of lake level rise 1986 versus 2002 from the USGS water level gauge in Russell Fjord (modified from [Trabant *et al.*, 2003b]). Once dammed, the lake level rose at an average rate of about  $0.2 \text{ m d}^{-1}$  in both years. In 2002, rapid influx of water into the lake basin from heavy rains accelerated lake level rise to  $\sim 1 \text{ m d}^{-1}$ . The 2002 outburst occurred significantly sooner and at lower lake level than in 1986.

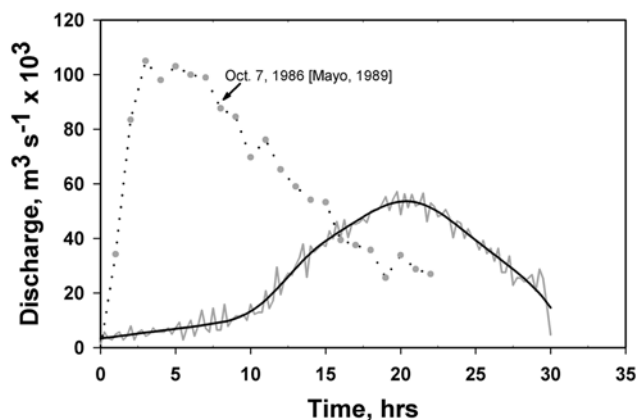


**Figure 6.** The 2002 outburst hydrograph (solid curves). The jagged curve is derived from lake level measurements, and the smoothed curve is the modeled discharge (section 5.1). The outburst record from 1986 is shown for comparison (dotted line).

divergence was visible at least 1 km upstream from the terminus. Increased flux to the east caused ice advance with ice almost crossing the gap behind the moraine dam (Figures 4 and 7b).

[26] The time interval for vectors in Figure 7c spans only 2 days, from ~1630 on August 14, during the peak of the outburst to ~1630 August 16, only a day after the flood had dissipated. Figure 7c thus captures the major reorganization that ice underwent during this 2-day period in response to the rapidly changing conditions at Gilbert Point. Within this short time interval ice flowing into EDB doubled in speed from 5–6 m d<sup>-1</sup> to preclosure speeds of 11–12 m d<sup>-1</sup> and flowed in a more westerly direction. However, ice flow upstream of the dam was apparently still readjusting to changes in terminus boundary conditions with speeds and directions at or below uncertainty levels (<1–3 m d<sup>-1</sup>). The gradient between terminus and up-glacier velocities shows that the near-terminus ice was being subjected to strong extensional forces during the outburst.

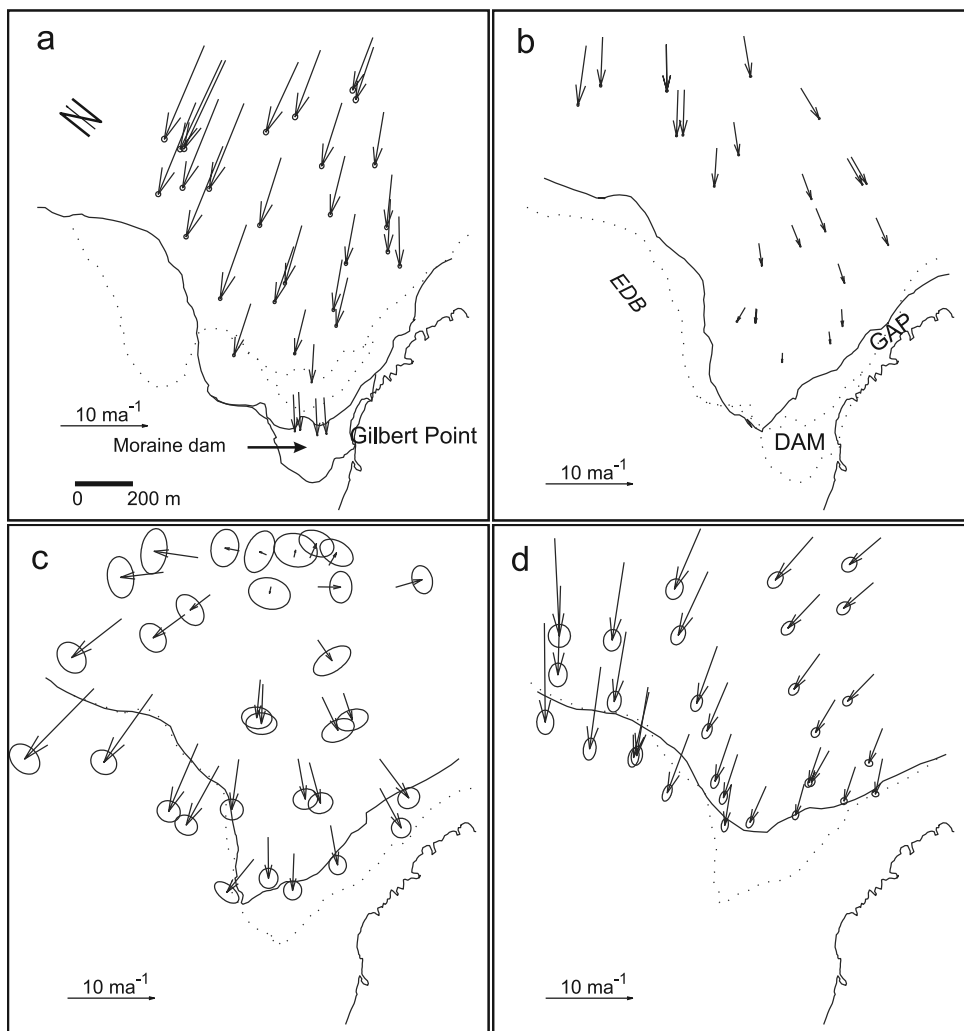


**Figure 7.** Surface ice velocities near Gilbert Point determined from vertical aerial photos: (a) 7 June to 7 July, (b) 7 July to 14 August, (c) 14–16 August, and (d) 16–23 August. Dashed (solid) line shows glacier boundary from the first (second) photo date in each plot. Moraine dam is shown in Figures 7a and 7b.

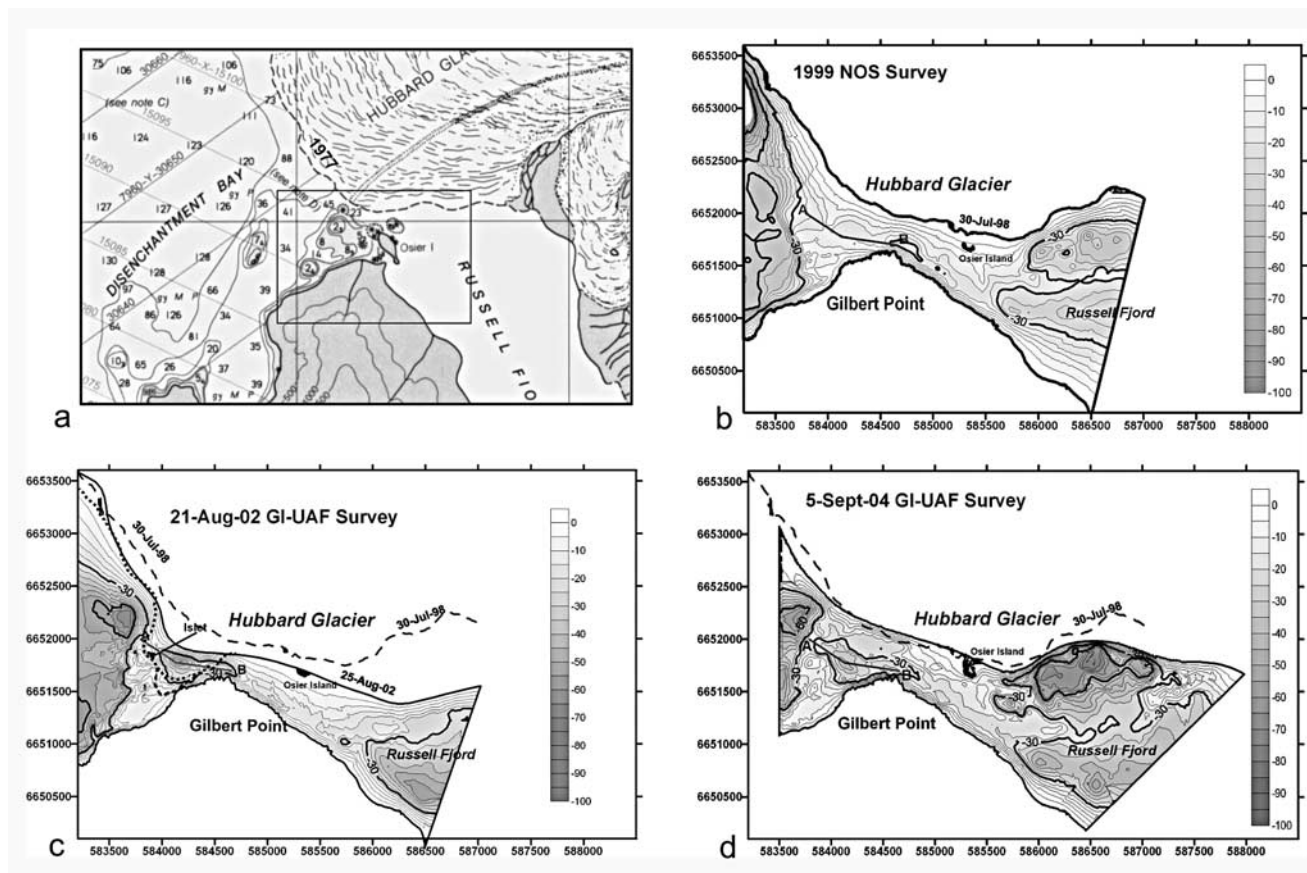


**Figure 8.** Bathymetric surveys of Gilbert Point channel. (a) Portion of NOAA Chart 16761 showing channel as it looked in 1977–1978, depths in fathoms. For surveys in Figures 8b, 8c, and 8d, depths are in meters with 5 m contour interval, and coordinates are UTM, NAD 83 zone 7. (b) Channel depths from 1999 NOAA hydrographic survey. (c) Channel depths immediately following 2002 outburst flood. The lateral extent of the 7 July 2002 ice and moraine dam (short-dashed lines) is also shown. (d) Channel depths 2 years after outburst. Thick line (A–B) near midchannel on Figures 8b, 8c, and 8d marks cross-section location for Figure 9.

[27] Over the next 8 days following the outburst the strong extensional conditions rapidly diminished as upstream ice increased in speed (Figure 7d). The post outburst ice flow regime overall appears to have resumed its predam pattern, with velocity gradients and directions similar to Figure 7a.

#### 4.4. Gilbert Point Bathymetry

[28] Bathymetric charts of the Gilbert Point area derived from the NOS 1977 and 1999 surveys and from our own surveys in 2002 and 2004 are shown in Figure 8. Because of inherent dangers associated with a calving face, we remained at least 100 m or farther from terminus ice cliffs NOS surveys were even more conservative, keeping at least 0.25 km from calving faces. Contours near the ice cliffs are therefore extrapolated from the nearest soundings.

[29] A cross section of submarine topography in the channel based on the 1999 and 2002–2005 annual bathymetric surveys is shown in Figure 9. Post outburst bathymetry documented that the glacier advance and the flood eroded the channel to depths of 60 m at Gilbert Point (Figures 8c and 9). However, a 1-km-long, 300-m-wide

submerged sill to the west of Gilbert Point appears on NOS 1999 bathymetry and persists on all of our post-2002 outburst bathymetry (Figure 8). The persistence of this sill despite outburst floods suggests that it is an erosion-resistant bedrock reef. The sill rises to within 10 m below MLLW and extends northward toward the glacier terminus.

#### 4.5. Water Temperatures

[30] Late summer ocean temperatures in EDB were warm and similar for 2002–2005, and showed a positive gradient with depth, increasing from 6.5°C near the surface to as much as 10.4°C at depths of 50 m (Figure 10). Spring temperatures in EDB on 25 April 2003 were considerably cooler, averaging 5.4°C and show little change with depth. Late summer 2004 Russell Fjord water temperatures were comparatively uniform throughout the measured water column, averaging about 7°C.

[31] Our limited temperature record suggests ocean temperatures in EDB undergo a seasonal variation, particularly at 50 m depth (Figure 10). Additional evidence for seasonal warming at these depths comes from *Reeburgh et al.* [1976], who reported temperatures in EDB ranging from a

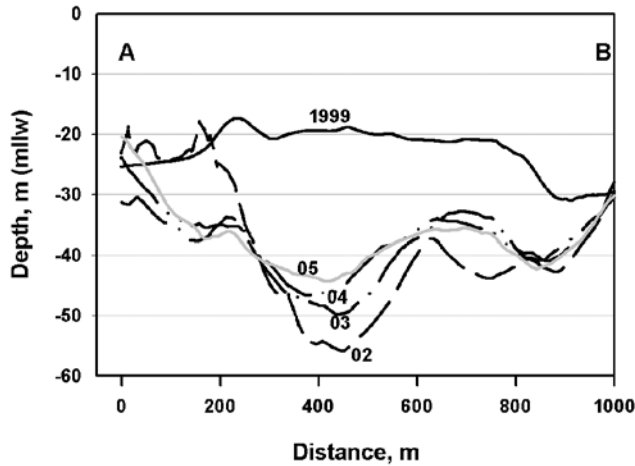


**Figure 9.** Bed profiles taken along the channel of maximum depth west of Gilbert Point where all surveys had adequate data (line A–B in Figure 8).

minimum of 2.75°C in March–April to a maximum of 7°C in late August–September in 1973.

## 5. Discussion

### 5.1. Discharge Hydrograph and Model

[32] While the 1986 outburst was largely the result of an ice dam failure, the 2002 event was controlled by downward erosion of a moraine, lateral erosion into glacier ice, and glacier calving. This difference is reflected in the discharge curves (Figure 6): the time to peak flow exceeded 20 hours in 2002, and peak discharge was less than half of that observed in 1986. A physically based discharge model of the 2002 event needs to account for the widening of the channel as well as its deepening. We therefore adopted *Walder and Costa's* [1996] (hereinafter referred to as WC96) model of outbursts from glacier-dammed lakes to describe the widening of the channel and combined it with *Walder and O'Connor's* [1997] (hereinafter referred to as WO97) model of failures of earthen dams to describe the moraine failure. A further complication in the Hubbard event is that moraine erosion continued to below sea level. Assuming a constant sediment erosion rate  $k$ , the governing equations (equations (25) and (27) in WC96) become:

$$\begin{aligned} dB/dt = & -u_i + u_c + 0.068(\rho_w/\rho_i)(f_R/L')(gh)^{3/2} \\ & + 0.226 k_w(\theta_o - \theta_i)/(\rho_i L') \\ & \cdot \left\{ g^{1/2} \rho_w B h^{1/4} / [\eta_w(4h/3 + B)] \right\}^{4/5} \end{aligned} \quad (2)$$

$$2/3(A_o + w/w_i \Delta A) dw/dt = Q_i - (2/3)^{3/2} g^{1/2} B h^{3/2} \quad (3)$$

where

$$h = w - w_i - k t \quad (4)$$

and where  $\Delta A$  is the difference in lake area between the filled lake and the lake when it is back at sea level. This

corresponds to WC96's "minimum model (i.e., only local dissipated energy contributes to the melting of the ice wall). Here,  $B$  is the width of the breach,  $u_i$  is the ice flow speed,  $u_c$  the calving speed,  $\rho_w$  and  $\rho_i$  are the densities of water and ice,  $f_R$  is a friction coefficient,  $L'$  the latent heat of fusion,  $g$  the gravitational acceleration,  $k_w$  the thermal conductivity of water,  $\theta_o$  and  $\theta_i$  are the water and ice temperatures,  $\eta_w$  is the viscosity of water, and  $Q_i$  is the water inflow into the lake. Equation (2) is different from WC96's equation 27, because we adopt a different approximation for the volume change of the lake (see below). In equations (2)–(4),  $h$  is the water level above the top of the dam,  $w$  is the water level with respect to sea level (Figure 11),  $w_i$  is the initial water level,  $k$  the downward erosion rate of the moraine (presumed constant here), and  $t$  the time since the start of the outburst. Equations 2 and 3 have to be slightly modified if moraine erosion proceeds to below sea level (see below).

[33] We solved the coupled equations (2)–(4) for  $B(t)$  and  $w(t)$  using the Matlab ODE solver. In the absence of calving ( $u_c = 0$ ) lateral erosion of the glacier dam is substantially slower than the average of 7 m h<sup>-1</sup> observed during the event (Table 1), even when accounting for the relatively high water temperatures of 7°C, observed in Russell Fjord (section 4.5). This is consistent with results from WC96 who described outburst events lasting several days. Obviously, the lateral expansion of the channel was determined by ice calving rather than melting. Solving the coupled equations (2)–(4) and attempting to fit  $w(t)$  to observations also revealed that sediment erosion rates in the moraine were quite slow (compared to typical values listed in WO97) and that these rates are not constant.

[34] We therefore adopted a different approach and attempted to derive sediment erosion rates using the water level data and a model for water discharge, rather than tuning the rates in an attempt to fit observations. We use the same geometric variables as above (Figure 11), with the

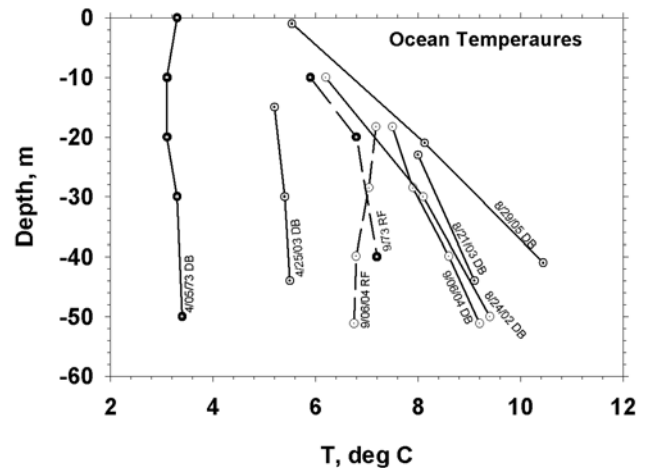


**Figure 10.** Water temperatures in Disenchantment Bay and Russell Fjord. Dates of measurements adjoin curves. Open circles are measurements from this study. Solid circles are from *Reeburgh et al.* [1976]. DB, Disenchantment Bay (solid lines); RF, Russell Fjord (dashed lines).

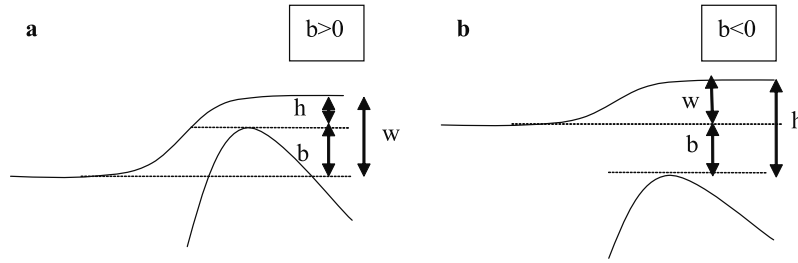


**Figure 11.** Schematic geometry of the outburst dam with (a) the moraine above sea level and (b) the moraine below sea level. Here  $w$  is the lake water level with respect to sea level,  $b$  is the position of the top of the moraine dam with respect to sea level, and  $h$  is the water level with respect to the top of the moraine.

addition of  $b$ , which is the position of the top of the moraine with respect to sea level. Therefore

$$w = b + h \quad (5)$$

Here we assume that sediment erosion proceeds at a nonconstant rate  $k$  (guided by our initial modeling results):

$$b(t) = w_i - \int_{t_0}^t k(t) dt \quad (6)$$

[35] The outflow  $Q$  is given by the average velocity  $u$  multiplied with the cross section, which we assume to be rectangular. We follow WC96 (their equation (8)) and assume critical flow:

$$u_{>} = (2/3 g h)^{1/2} \quad (7a)$$

$$u_{<} = (2/3 g w)^{1/2} \quad (7b)$$

Equation (7a) refers to  $b > 0$  and 7b to  $b < 0$ . We use the subscript  $>$  and  $<$  to distinguish the two cases from here on. The distinction is necessary, because only the difference between lake and sea level drives flow when the moraine height is below sea level. The factor of 2/3 derives from an effective breach height, as discussed by WC96 (their equation (7)). The discharge  $Q$  can now be written as

$$Q_{>} = B h (2/3)^{3/2} (g h)^{1/2} \quad (8a)$$

$$Q_{<} = B h (2/3)^{3/2} (g w)^{1/2} \quad (8b)$$

Using  $h = w - b = w - w_i + \int k dt$  we obtain

$$Q_{>} = B (2/3)^{3/2} g^{1/2} \left( w - w_i + \int_{t_0}^t k(t) dt \right)^{3/2} \quad (9a)$$

$$Q_{<} = B (2/3)^{3/2} g^{1/2} \left( w - w_i + \int_{t_0}^t k(t) dt \right) w^{1/2} \quad (9b)$$

[36] Our initial modeling showed, in agreement with WC96, that lateral melting is very slow and is negligible during the duration of the flood. Instead we use an approx-

imation to the observed widening of the channel, i.e., an initial blowout to a 60 m width and then a linear increase in  $B$  at the rate of 7 m h<sup>-1</sup>.

[37] The discharge can now be related to the rate of change of lake water volume:

$$dV/dt = Q_i - Q \quad (10)$$

where  $Q_i$  is the inflow into the lake ( $\sim 1000 \text{ m}^3 \text{ s}^{-1}$ ). The volume of the lake  $V$  can be given as a function of water level  $w$ . Here we do not follow WC96's equation (10) but instead approximate the rate of change of lake volume as that of a prism of height  $w + x$ , following the hypsometry of Mayo [1989]:

$$V = 1/3 A(w)(w + x) \quad (11)$$

[38] We assume that the area  $A = A_0 + w/w_i \Delta A$  is a linear function of  $w$  [Mayo, 1989] and  $x = w_i A_0 / \Delta A$  is the extrapolated depth at which the lake area would vanish ( $A(-x) = 0$ ).  $A_0$  is the lake area at  $w = 0$ , and  $A_0 + \Delta A$  is the lake level at  $w = w_i$ . The rate of volume change is therefore given by

$$dV/dt = 2/3 (A_0 + w/w_i \Delta A) dw/dt \quad (12)$$

Equations 9a and 12 can now be combined to find

$$\int_{t_0}^t k_{>} dt = \left\{ \left[ (2/3)^{3/2} g^{1/2} B \right]^{-1} \cdot [Q_i - 2/3 (A_0 + w/w_i \Delta A) dw/dt] \right\}^{2/3} + w_i - w \quad (13a)$$

$$\int_{t_0}^t k_{<} dt = \left[ (2/3)^{3/2} g^{1/2} B^{1/2} w^{1/2} \right]^{-1} \cdot [Q_i - 2/3 (A_0 + w/w_i \Delta A) dw/dt] + w_i - w \quad (13b)$$

Using the fundamental theorem of calculus and some algebra we now find

$$k_{>} = -g^{1/3} [Q_i - 2/3 (A_0 + w/w_i \Delta A) dw/dt]^{2/3} \cdot \left\{ B^{-5/3} dB/dt + 2/3 B^{-2/3} \cdot [Q_i - 2/3 (A_0 + w/w_i \Delta A) dw/dt]^{-1} \cdot [(A_0 + w/w_i \Delta A) d^2 w/dt^2 + \Delta A/w_i (dw/dt)^2] \right\} - dw/dt \quad (14a)$$

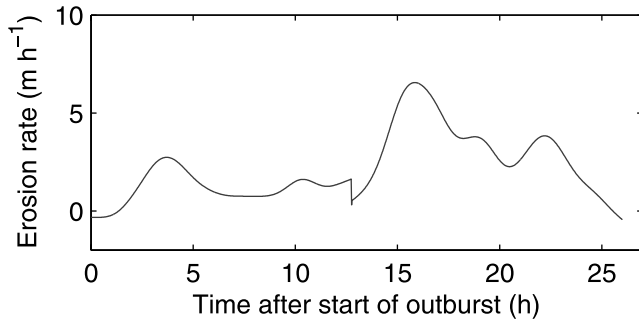


**Figure 12.** Dam erosion rates derived from the water level record. Increased rates occur about 13 hours after dam failure starts. Around that same time, dam erosion proceeds to below sea level, and ice calving enlarges the channel laterally.

$$\begin{aligned}
 k_{<} = & - (2/3)^{-3/2} g^{-1/2} B^{-1} w^{-1/2} \\
 & \cdot \left\{ (dB/dt) B^{-1} + 1/2 w^{-1} dw/dt \right\} \\
 & \cdot [Q_i - 2/3 (A_0 + w/w_i \Delta A) dw/dt] \\
 & + 2/3 \left[ (A_0 + w/w_i \Delta A) d^2 w/dt^2 + \Delta A/w_i (dw/dt)^2 \right] - dw/dt
 \end{aligned} \tag{14b}$$

[39] The calculation of  $k$  was done with a smoothed water level record to avoid too much noise in  $dw/dt$  and particularly in  $d^2w/dt^2$ . We obtained sediment erosion rates of  $\sim 1\text{--}2 \text{ m h}^{-1}$ , temporarily increasing to  $\sim 6 \text{ m h}^{-1}$  (Figure 12). These rates are much lower than the typical  $10\text{--}100 \text{ m h}^{-1}$  reported by WO97. Interestingly, observations and modeling results show different events happening near simultaneously: (1) the start of ice calving, (2) the moraine beginning to erode to below sea level, and (3) moraine erosion rates increasing. This happened roughly 13 hours after the start of the outburst. The discontinuity of the calculated erosion rates is due to a discontinuity in  $dB/dt$ , because, as described above,  $B$  was assumed constant until ice calving started and to then increase linearly afterward. The derived sediment erosion rates are quite robust with regards to the various parameters in equations (14a) and (14b). However,  $d^2w/dt^2$  is a numerical derivative that gets very noisy. We addressed this by smoothing the record with a Gaussian of half-width 40 min. Variations of erosion rates on shorter timescale cannot be expected to be resolved with this method.

## 5.2. Temporal and Spatial Changes in Ice Flow

[40] The rapidity of ice flow adjustment to changing conditions at Gilbert Point is striking. During the initial stages of 2002 dam formation, ice speeds and flow patterns were nearly identical to those reported for flow in this region for summer 2001 [Trabant *et al.*, 2003a; R. M. Krimmel, unpublished data, 1990s]. These speeds were quite high, ranging from 12 to  $4 \text{ m d}^{-1}$  in a N – S gradient. Given that ice thickness within 1 km of the terminus was likely 200 to 400 m [Trabant *et al.*, 1991], most ( $\geq 90\%$ ) of the measured surface ice velocity must be attributable to basal sliding. Thus any changes blocking basal sliding would be immediately reflected in the surface velocity.

[41] As the moraine moved forward and began colliding with Gilbert Point, the boundary conditions for upstream ice changed appreciably. With the terminus impeded and no longer free to simply slide forward, sliding was substantially reduced. The new flow barrier caused ice divergence to both sides of Gilbert Point and a zone of compression behind the ice front with strain rates of about  $-3.5 \times 10^{-3} \text{ d}^{-1}$ . Ice incompressibility would demand that most of this compression resulted in ice thickening. If ice thickness was on the order of 100 to 200 m in that area, local thickening rates could have been of the order of  $0.35\text{--}0.70 \text{ m d}^{-1}$ . Only a small portion of this thickening would have been offset by summer ablation, which for coastal regions can average  $0.05 \text{ m d}^{-1}$  [Motyka *et al.*, 2002; Boyce *et al.*, 2007].

[42] The flow divergence increased flux east of Gilbert Point, which led to ice advance there and ice almost crossed the gap in August (Figures 4 and 7b). If this had occurred, thickening ice could have significantly increased the height of the dam, and possibly made it less susceptible to the ensuing August rain event. Instead, flood waters from intense rains rapidly eroded the dam and submarine sediments, widening and deepening the channel. With the barrier to basal sliding removed, the terminus ice immediately responded to these new conditions and quickly accelerated. This acceleration resulted in strong extensional strain rates, which probably fractured and weakened the ice, thus contributing to the calving collapse and channel widening during and following the flood.

[43] In the 10 day period following the outburst, upstream ice speeds increased to predam levels and flow generally returned to its predam pattern of flow.

## 5.3. Temporal and Spatial Changes in Submarine Topography

[44] Both the 1986 and 2002 outburst floods substantially and rapidly altered the submarine terrain in the Gilbert Point region, stripping massive amounts of ice, sediments (and perhaps bedrock), redepositing them in Disenchantment Bay [Cowen *et al.*, 1996]. The first bathymetry of the Gilbert Point area after the 1986 outburst was made 2 years later in July 1988 [Trabant *et al.*, 1991]. These soundings were sparse but suggest scoured depths exceeded 35 m. In subsequent years, the glacier likely modified submarine topography by remobilizing and excavating glaciomarine sediments, redepositing them in proglacial areas [e.g., Hunter *et al.*, 1996; Motyka *et al.*, 2006]. Our post 2002 outburst bathymetry showed the existence of a shallow erosion-resistant sill west of Gilbert Point (Figure 8). We believe that this sill acted as a sediment trap following 1986 and sediment accumulation behind the trap helped gradually fill the channel (see 1999 bathymetry, Figure 8b). By 2002 the sediments had presumably become so shallow that the spring advance was able to push these sediments upward above sea level, thereby cutting off calving, and also forward onto and partially overriding the sill during the closure (Figure 8). Our examination of photos shows that this rapid closure was facilitated in part by development of a series of imbricate thrust faults within the moraine, similar to those observed at Taku Glacier, another strongly advancing glacier south of Juneau, Alaska [Motyka and Echelmeyer, 2003; Kuriger *et al.*, 2006].

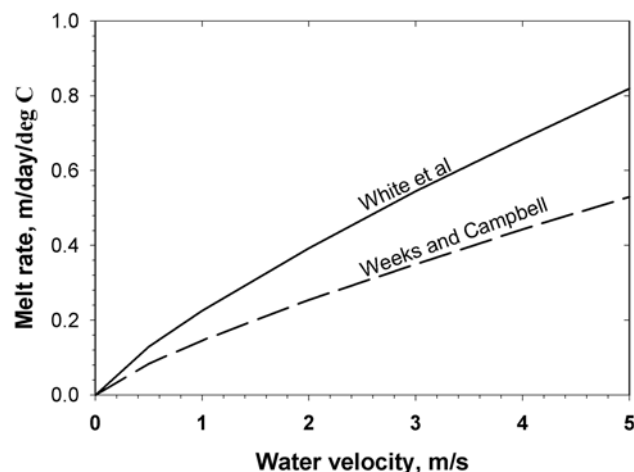


**Figure 13.** Estimate of submarine melt rate in meters per day per degree Celsius above melting point as a function of water velocity based on equations from *Weeks and Campbell* [1973] and *White et al.* [1980].

[45] Our bathymetric surveys show that following the 2002 outburst the channel was scoured to depths of 60 m by the outburst flood and ice advance. However, during the outburst, the sill remained intact, deflecting flow toward the glacier front, creating a deep channel there. Since the 2002 outburst, the sill appears to be again acting as a sediment trap. The scoured basin east of this sill is gradually filling in with sediment at a rate of about  $4 \text{ m yr}^{-1}$  although in 2005 the channel was still about 25 m deeper than in 1999 (Figure 9). Sediment accumulation will help reduce calving [e.g., *Brown et al.*, 1982], thus enhancing conditions for sustained glacier advance and push moraine development and therefore for another closure.

#### 5.4. Calving and Submarine Melting

[46] Between 1986, and 2002 the rate of glacier advance averaged  $\sim 30 \text{ m yr}^{-1}$  everywhere along the terminus except at Gilbert Point. There, the advance averaged only  $6 \text{ m yr}^{-1}$ . Had the glacier at Gilbert Point advanced as rapidly as elsewhere, the next closure would have occurred within less than a decade, as *Trabant et al.* [1991] predicted, rather than 16 years later. Since 2002 the annually averaged terminus position at Gilbert Point has remained nearly constant at about 350 m from Gilbert Point, despite the fact that the advance into Disenchantment Bay has continued at  $\sim 30 \text{ m yr}^{-1}$ . In addition, the Gilbert Point terminus has advanced 100 m or more in the spring, only to retreat during the summer, well before the gap could be breached. Three questions arise from these observations: (1) What conditions prevent the glacier at Gilbert Point from advancing as rapidly as elsewhere? (2) What conditions and events precipitated the eventual closure in 2002? (3) What drives the seasonal changes in terminus position?

[47] The answers to these questions are related to tidewater glacier dynamics, specifically calving and submarine melting. The latter in turn are related to the water depth in the channel, the seasonal changes in ocean water temperature, and tidal currents in the channel. At the Gilbert Point gap, tidal currents can reach several meters per second. As long as a water channel and tidal currents remain along the

calving face, the terminus is likely to experience submarine melting, with the magnitude increasing through the summer as water temperature increases. Such submarine thermal undercutting naturally leads to mechanical calving of the subaerial face [*Hanson and Hooke*, 2000]. To obtain estimates of this submarine melting, we used two equations originally derived for submarine melting of icebergs. The first was developed by *Weeks and Campbell* [1973] for the melting of an iceberg towed at a relative speed of  $u$  ( $\text{m s}^{-1}$ ), which incorporates forced convection and turbulent flow along the submerged face. The melt rate is given by

$$V_m = 6.74 \times 10^{-6} u^{0.8} T/l_i \quad (15)$$

where  $l_i$  is a characteristic ice length (water line length of the iceberg) and the melt rate,  $V_m$ , is in  $\text{m s}^{-1}$ . Here we take ice to be temperate and the ocean temperature to be  $T$  ( $^{\circ}\text{C}$ ) and treat  $u$  as the water velocity along the submerged terminus ice front.

[48] *White et al.* [1980] also developed approximate solution for turbulent flow past tabular icebergs:

$$V_m = 0.055 \text{Re}^{0.8} \text{Pr}^{0.4} k (T/l_i)(1/\rho_i L) \quad (16)$$

[49]  $\text{Re}$  and  $\text{Pr}$  are the Reynolds and Prandtl numbers, respectively,  $k$  is the thermal conductivity,  $\rho_i$ , the density of ice,  $L$ , the latent heat of fusion, and  $V_m$  is again in  $\text{m s}^{-1}$ . At Hubbard Glacier, water temperatures can fluctuate from as low as  $3^{\circ}\text{C}$  in early spring to as much as  $10^{\circ}\text{C}$  in late summer depending on water depth (Figure 10). We have not measured tidal currents in the channel but our qualitative observations during bathymetry surveys suggest that they can reach several  $\text{m s}^{-1}$  at maximum flood and ebb. We take the characteristic length to be  $\sim 1 \text{ km}$ , the approximate distance from the sill to Osier Island where the channel is the narrowest and currents strongest, and where past closures have occurred (Figure 8).

[50] Figure 13 plots the results for the above equations and our assumed values and gives the estimated melting rates. Equation (16) predicts somewhat higher melt rates than equation (15). If we assume a conservative value of  $\sim 3 \text{ m s}^{-1}$  for the daily average tidal current through the gap, and use the average of the two values for melt rate from Figure 13, we find that melt rates in the channel could range from a low of  $1.3 \text{ m d}^{-1}$  in early spring ( $3^{\circ}\text{C}$ ) to as much as  $4.5 \text{ m d}^{-1}$  in late summer ( $10^{\circ}\text{C}$ ), compared to average ice velocity of about  $5 \text{ m d}^{-1}$  along this section of the terminus. We in fact observed undercutting of freshly calved ice faces at the water line by a meter or more over a period of a few hours during our late-summer bathymetric surveys at Gilbert Point. Although we do not discount seasonal changes in ice speed as contributing to seasonal oscillations of the terminus position, we believe that the threefold increase in seasonal submarine thermal erosion could also reasonably explain the seasonal changes in terminus through increased submarine melting and calving. Similar seasonal temperature changes of seawater correlated with seasonal changes in terminus position have been observed at LeConte Glacier [*Motyka et al.*, 2003], at Columbia Glacier [*Walters et al.*, 1988], and at other Alaskan fjords and bays with tidewater glaciers [e.g., *Hooge and Hooge*, 2002].

[51] The combination of deep channel, strong tidal currents and warm ocean temperatures can similarly account for the reason the terminus has failed to cross the gap and close the fjord. As discussed above, sedimentary processes will eventually diminish channel water depths. Once moraine material is pushed above water in front of a seasonally advancing terminus, it will effectively isolate the ice front from the ocean and thereby shut down the calving and submarine processes, allowing the glacier to advance unabated.

### 5.5. Future Closures

[52] The continued advance of Hubbard Glacier guarantees that Russell Fjord will be closed again [Trabant *et al.*, 1991; 2003a]. An often-referenced empirical AAR (accumulation to total area ratio) value for a glacier in steady state is 0.65–0.70 [Paterson, 1994]. If Hubbard were to advance until it reached this state with the current equilibrium line altitude (ELA), the advance would continue down Disenchantment Bay for over 30 km, and would last for over 1000 years at the current advance rate of  $\sim 30$  m yr<sup>-1</sup>. Continuation of the glacier's expansion is unlikely to change in the near future as a result of further climate change. Currently the ELA is located in a fairly steep area. Raising the ELA by 100 m only changes the AAR to 0.92. Furthermore, the glacier has an accumulation area that extends to very high altitudes and there are some indications of recent increased precipitation rates at high altitudes on nearby Variegated Glacier [Eisen *et al.*, 2001].

[53] We believe the key to the next closure is halting the process of submarine melting and mechanical calving as discussed above. Thus we propose that future closures will depend in part on continued sedimentation into the channel at Gilbert Point. After 1986, the channel gradually filled in with sediments derived from glacier erosion and remobilization of sediments by glacier advance. The reef west of Gilbert Point probably helped to trap these sediments. By spring 2002, a subaerial push moraine developed as a result of shallow water, mobile sediments, and seasonal advance. This shoal moraine succeeded in isolating the terminus from ocean water and channel currents, substantially reducing or eliminating submarine melting and calving losses, allowing the fjord to be closed. The 2002 outburst scoured the channel to depths of 60 m. We suspect that sediments must again accumulate to a sufficient level before another closure can take place because deep water inhibits glacier advance due to the effects of calving and submarine melting. Given the current rates of sediment accumulation it may take another ten years for sediments to fill the gap to 1999 levels (Figure 9).

[54] Complicating this prediction are ice flow instabilities. While Hubbard Glacier is not known to surge, many of its tributaries do. Such surges or other flow instabilities can temporarily increase ice velocities of the main trunk glacier, and Mayo [1989] suggested that the 1986 closure may have been triggered in part by a weak surge of the Valerie tributary. Some tributaries of the glacier were also reported to have surged in 2001/02 (K. Echelmeyer, personal communication, June 2002) so perhaps surges could have been a contributing factor during the 2002 closure, although direct evidence is lacking. In fact, there was no anomalously high rate of advance anywhere else along the terminus in 2002

that would suggest a surge. However, a future surge, if powerful enough, could drive the terminus across even a deep water channel.

## 6. Conclusions

[55] In 2002, a spring ice advance near Gilbert Point pushed shallow submarine proglacial sediments above water, isolating a 1-km-long section of the terminus from deep ocean water and strong tidal currents. This moraine was pushed against Gilbert Point and by late June, closed off Russell Fjord. Upstream ice flow rapidly decelerated from 5 m d<sup>-1</sup> to 1.5 m d<sup>-1</sup> and flow diverged to either side of Gilbert Point. Vertical growth of the moraine dam outpaced lake level rise with the height eventually reaching 15 m asl. However, three days of intense rain caused lake water to overtop the dam on 14 August 2002. The flood waters rapidly eroded sediments and ice causing the channel to widen to 230 m and deepen to as much as 60 m bsl. 3 km<sup>3</sup> of water were released within 30 hours with peak discharge reaching 55,000 m<sup>3</sup> s<sup>-1</sup>, 24 hours after the flood began. The loss of buttressing against Gilbert Point caused upstream ice to quickly accelerate (to 5 m d<sup>-1</sup>). Flow changed direction toward Disenchantment Bay with the flow pattern returning to predam conditions within a few days of the outburst.

[56] The discharge records for the 1986 and 2002 outbursts differ significantly and reflect differences in lake height ( $\pm 26$  m versus 15 m) and dam types (ice versus moraine). A simple model of the outburst indicates that moraine erosion rates were almost an order of magnitude slower than those reported by Walder and Costa [1996] for other earthen dams. The outburst proceeded essentially in two stages: (1) relatively slow overtopping of the subaerial moraine and downward erosion at rates of 1–2 m h<sup>-1</sup> with little amounts of lateral expansion due to ice calving, and (2) faster downward erosion of the submarine moraine (up to 7 m h<sup>-1</sup>) with a lateral expansion of the channel due to significant ice calving ( $\sim 7$  m h<sup>-1</sup>).

[57] The annual average terminus position at Gilbert Point has remained relatively constant since 2002 despite the fact that the rest of the terminus continues to advance at rates of  $\sim 30$  m yr<sup>-1</sup>. Seasonal variations of up to 200 m have been also been observed. We attribute these anomalies and the fact that 16 years elapsed between closures to submarine melting and mechanical calving driven by seasonal changes in water temperature and to a deep water channel. However, sediments are slowly filling in the Gilbert Point gap behind an erosion resistant sill at a rate of about 4 m yr<sup>-1</sup>. Their steady accumulation may eventually trigger the next closure. At the current rate of sediment infilling, it may take another ten years before waters shallow to depths equivalent to the pre-2002 event. However, glacier instabilities such as surges of tributaries could trigger an anomalously rapid advance and close Russell Fjord at any time regardless of water depth. Thus monitoring of both bathymetry and glacier dynamics is warranted. This is of critical concern to local residents as a future closure could produce overflow and flooding south of Russell Fjord, potentially damaging lucrative fisheries and village infrastructures. Outbursts of the magnitude seen in the past from Russell Fjord also constitute a severe hazard to navigation in the bay.

[58] **Acknowledgments.** Support for this work was provided in part by U.S. National Science Foundation grant OPP-0221307, by NASA grant NAG5-13760, and by U.S. National Park Service grant G-2276. Additional support was provided by the Geophysical Institute, University of Alaska. We wish to thank R. Johnson and the AK Department of Fish and Game for their generous logistics support, R. Gubernick (USDA Forest Service) for sharing lidar data, the USDA Forest Service, Yakutat District, the U.S. National Park Service, Yakutat office, and the people of Yakutat for sharing their photos and observations, and the U.S. National Marine Fisheries Service for providing us with digital copies of their summer 2002 vertical aerial coverage of Hubbard Glacier terminus. We would also like to thank following individuals for valuable field assistance: Jackie Lott (USNPS), By Valentine, Ned Rozell, and Michael Hekkers. Brent Ritchie contributed Figure 2. The manuscript greatly benefited by reviews from N. Iverson, J. Walder, M. Funk, and H. Björnsson.

## References

- Anderson, S. P., J. S. Walder, R. S. Anderson, E. R. Kraal, M. Cunico, A. G. Fountain, and D. C. Trabant (2003), Integrated hydrologic and hydrochemical observations of Hidden Creek Lake jökulhlaups, Kennicott Glacier, Alaska, *J. Geophys. Res.*, *108*(F1), 6003, doi:10.1029/2002JF000004.
- Arendt, A. A., K. A. Echelmeyer, W. D. Harrison, C. S. Lingle, and B. Valentine (2002), Rapid wastage of Alaska glaciers and their contribution to rising sea level, *Science*, *297*, 382–386.
- Barclay, D. J., P. E. Calkin, and G. C. Wiles (2001), Holocene history of Hubbard Glacier in Yakutat Bay and Russell Fiord, southern Alaska, *Geol. Soc. Am. Bull.*, *113*, 388–402.
- Björnsson, H. (1992), Jökulhlaups in Iceland: Prediction, characteristics, and simulation, *Ann. Glaciol.*, *16*, 95–106.
- Björnsson, H. (2002), Subglacial lakes and jökulhlaups in Iceland, *Global Planet. Change*, *35*, 255–271.
- Boyce, E. S., R. J. Motyka, and M. Truffer (2007), Flotation and retreat of a lake-calving terminus, Mendenhall Glacier, southeast Alaska, *J. Glaciol.*, in press.
- Brown, C. S., M. F. Meier, and A. Post (1982), Calving speed of Alaska tidewater glaciers, with application to Columbia Glacier, *U.S. Geol. Surv. Prof. Pap.*, *1258-G*.
- Cowen, E. A., P. R. Carlson, and R. D. Powell (1996), The marine record of the Russell Fiord outburst flood, Alaska, USA, *Ann. Glaciol.*, *22*, 194–200.
- Eisen, O., W. D. Harrison, and C. F. Harrison (2001), The surges of Variegated Glacier, Alaska, U. S. A., and their connection to climate and mass balance, *J. Glaciol.*, *47*(158), 351–358.
- Hanson, B., and R. L. Hooke (2000), Glacier calving: A numerical model of forces in the calving-speed–water-depth relation, *J. Glaciol.*, *46*(153), 188–196.
- Hooge, P. N., and E. R. Hooge (2002), Fiord oceanographic processes in Glacier Bay, Alaska, report, 142 pp., Alaska Sci. Cent., U.S. Geol. Surv., Anchorage.
- Hunter, L. E., R. D. Powell, and D. E. Lawson (1996), Flux of debris transported by ice at three Alaskan tidewater glaciers, *J. Glaciol.*, *42*(140), 123–135.
- Krimmel, R. M. (2001), Photogrammetric data set, 1957–2000, and bathymetric measurements for Columbia Glacier, Alaska, *U.S. Geol. Surv. Water Res. Invest. Rep.*, *WRIR 01-4089*, 40 pp. with CD-ROM.
- Krimmel, R. M., and D. C. Trabant (1992), The terminus of Hubbard Glacier, Alaska, *Ann. Glaciol.*, *16*, 151–157.
- Kuriger, E. M., M. Truffer, R. J. Motyka, and A. K. Bucki (2006), Episodic reactivation of large-scale push moraines in front of the advancing Taku Glacier, Alaska, *J. Geophys. Res.*, *111*, F01009, doi:10.1029/2005JF000385.
- Larsen, C. F., R. J. Motyka, A. Arendt, and K. A. Echelmeyer (2007), Glacier changes in southeast Alaska and northwest British Columbia and contribution to sea level rise, *J. Geophys. Res.*, *112*, F01007, doi:10.1029/2006JF000586.
- Mayo, L. R. (1988), Advance of Hubbard Glacier and closure of Russell Fiord, Alaska: Environmental effects and hazards in the Yakutat area, in *Geologic Studies in Alaska by the U.S. Geological Survey During 1987*, edited by J. P. Galloway and T. D. Hamilton, *U.S. Geol. Surv. Circ.*, *10016*, 4–16.
- Mayo, L. R. (1989), Advance of Hubbard Glacier and 1986 outburst of Russell Fiord, Alaska, U.S.A., *Ann. Glaciol.*, *13*, 189–194.
- Meier, M. F., and A. Post (1987), Fast tidewater glaciers, *J. Geophys. Res.*, *92*(B9), 9051–9058.
- Motyka, R. J., and K. A. Echelmeyer (2003), Taku Glacier on the move again: Active deformation of proglacial sediments, *J. Glaciol.*, *49*(164), 50–59.
- Motyka, R. J., S. O’Neel, C. Connor, and K. Echelmeyer (2002), 20th century thinning of Mendenhall Glacier, Alaska, and its relationship to climate, lake calving, and glacier run-off, *Global Planet. Change*, *35*(1–2), 93–112.
- Motyka, R. J., L. Hunter, K. A. Echelmeyer, and C. Connor (2003), Submarine melting at the terminus of a temperate tidewater glacier, LeConte Glacier, Alaska, *Ann. Glaciol.*, *36*, 57–65.
- Motyka, R. J., M. Truffer, E. M. Kuriger, and A. K. Bucki (2006), Rapid erosion of soft sediments by tidewater glacier advance: Taku Glacier, Alaska, USA, *Geophys. Res. Lett.*, *33*, L24504, doi:10.1029/2006GL028467.
- NOAA (1984), Yakutat Bay, Alaska, 13th ed., *Chart 16761*, scale 1:80000, Natl. Ocean Serv., Silver Spring, Md.
- NOAA (2000), Yakutat Bay, Alaska, 16th ed., *Chart 16761*, scale 1:80000, Natl. Ocean Serv., Silver Spring, Md.
- Paterson, W. S. B. (1994), *The Physics of Glaciers*, 3d ed., Elsevier, New York.
- Post, A. (1975), Preliminary hydrography and historic terminal changes of Columbia Glacier, Alaska, *U.S. Geol. Surv. Hydrol. Invest. Atlas*, *HA-559*, 3 maps, scale 1:10,000.
- Post, A., and R. J. Motyka (1995), Taku and LeConte Glaciers, Alaska: Calving speed control of late Holocene asynchronous advances and retreats, *Phys. Geogr.*, *16*, 59–82.
- Reeburgh, W. S., R. D. Muench, and R. T. Cooney (1976), Oceanographic conditions during 1973 in Russell Fiord, Alaska, *Estuarine Coastal Mar. Sci.*, *4*, 129–145.
- Ritchie, J., C. Lingle, M. Truffer, R. Motyka, A. Arendt, A. Prakash, K. Echelmeyer, and S. Zirnheld (2006), Seasonal and spatial variations in the advance of Hubbard Glacier, south-central Alaska, U.S.A., *Geophys. Res. Abstr.*, *8*, Abstract 06345.
- Roberts, M. J. (2005), Jökulhlaups: A reassessment of floodwater flow through glaciers, *Rev. Geophys.*, *43*, RG1002, doi:10.1029/2003RG000147.
- Seitz, H. R., D. S. Thomas, and B. Tomlinson (1986), The storage and release of water from a large glacier-dammed lake: Russell Lake near Yakutat, Alaska, 1986, *U.S. Geol. Surv. Open File Rep.*, *86-545*, 9 pp.
- Skvarca, P., and R. Naruse (2006), Correspondence—Overview of the ice-dam formation and collapse of Glacier Perito Moreno, southern Patagonia, in 2003/2004, *J. Glaciol.*, *52*(178), 476–478.
- Stuefer, M., H. Rott, and P. Skvarca (2007), Glacier Perito Moreno, Patagonia: Climate sensitivities and glacier characteristics preceding the 2003/04 and 2005/06 damming events, *J. Glaciol.*, *53*(180), 3–16.
- Trabant, D. C., R. M. Krimmel, and A. Post (1991), A preliminary forecast of the advance of Hubbard Glacier and its influence on Russell Fiord, Alaska, *U.S. Geol. Surv. Water Res. Invest.*, *90-4172*.
- Trabant, D. C., R. M. Krimmel, K. A. Echelmeyer, S. Zirnheld, and D. Elsberg (2003a), The slow advance of a calving glacier: Hubbard Glacier, Alaska, *Ann. Glaciol.*, *36*, 45–50.
- Trabant, D. C., R. S. March, and D. S. Thomas (2003b), Hubbard Glacier, Alaska: Growing and advancing in spite of global climate change and the 1986 and 2002 Russell Lake outburst floods, *U. S. Geol. Surv. Fact Sheet*, *001-03*.
- van der Veen, C. J. (1996), Tidewater calving, *J. Glaciol.*, *42*(141), 375–385.
- Walder, J. S., and J. E. Costa (1996), Outburst floods from glacier-dammed lakes: The effect of mode of lake drainage on flood magnitude, *Earth Surf. Processes Landforms*, *21*, 701–723.
- Walder, J. S., and J. E. O’Connor (1997), Methods for predicting peak discharge of floods caused by failure of natural and constructed earth dams, *Water Res. Res.*, *33*(10), 2337–2348.
- Walters, R. A., E. G. Josberger, and C. L. Driedger (1988), Columbia Bay, Alaska: An “upside down” estuary, *Estuarine Coastal Sci.*, *26*(6), 607–617.
- Weeks, W. F., and W. J. Campbell (1973), Iceberg as a freshwater source: An appraisal, *J. Glaciol.*, *12*(65), 207–223.
- White, F. M., M. L. Spaulding, and L. Gominho (1980), Theoretical estimates of the various mechanisms involved in iceberg deterioration in the open ocean environment, *Rep. CG-D-62-80 81-20571*, Coast Guard Res. and Dev. Cent., Groton, Conn.

R. J. Motyka and M. Truffer, Geophysical Institute, University of Alaska Fairbanks, 903 Koyukuk Drive, Fairbanks, AK 99775, USA. (jrfjm@uas.alaska.edu)